Proceedings of the 3rd International Conference on Fluid Flow and Thermal Science (ICFFTS'22)
~~Seoul, South Korea~~ Virtual Conference - October 27 - 29, 2022
Paper No. 118
DOI: 10.11159/icffts22.118

Noise Prediction of OSRVM Based on Steady-state Broadband Model

MinGyun Park[1], Ji-Hun Song[1], Youn-Jea Kim[2]
[1]Department of Mechanical Engineering, Sungkyunkwan University
Suwon 16419, South Korea
mg0112@g.skku.edu; sjh012@g.skku.edu
[2]School of Mechanical Engineering, Sungkyunkwan University
Suwon 16419, South Korea
*Corresponding author: yjkim@skku.edu

Abstract **–** The engine is the largest noise source in an internal combustion engine vehicle (ICV). The noise generated by the engine can cover the noise of other parts of the vehicle. This phenomenon is called the masking effect. Recently, the proportion of electric vehicles is gradually increasing. That means the engine disappears. With the disappearance of the engine, the importance of noise reduction, such as wind noise, cavity noise, and load noise are increasing. The biggest noise is the wind noise generated around the Outside Rear View Mirror (OSRVM). Wind noise is caused by pressure fluctuations in the unsteady flow field. flow simulation and noise simulation were performed based on the velocity change. In this study, Aeroacoustics was predicted based on the numerical analysis results, and the acoustic power level (APL) results of the reference model OSRVM and the modified modelled OSRVM were compared.

Keywords**:** Outside Rear View Mirror (OSRVM), Wind Noise, Flow Noise, Computational Fluid Dynamics (CFD), Computational Aeroacoustics (CAA).

1. Introduction

The development of automotive technology has improved the performance of automobiles. As the driving speed became higher than before, the noise caused by the wind took up a large proportion. Noise is subjective indicator that reflects the listener's psychology [1]. Noise related to vehicles includes mechanical noise generated by mechanical devices and aeroacoustics generated while driving. Aeroacoustics, as the name suggests, deals with the noise generated by the flow of fluid. The engine is the biggest noise source in an internal combustion engine vehicle. The noise generated by the engine could mask the noise generated by other automobile parts. The masking effect refers to a phenomenon in which small sounds cannot heard because of the loudest sound from the point of view of acoustic psychology. However, recently the automobile industry has faced a major paradigm shift from internal combustion engine vehicles (ICV) to electric vehicles (EV). The biggest change is that the engine does not exist. Other types of noise generated by automobiles include A-pillar vortex, wind noise, cavity noise, load noise, etc [2]. Due to this phenomenon, automobile drivers have increased their demand for aeroacoustics reduction. Among the many aeroacoustics, the noise that a driver can feel is wind noise generated by A-pillar and outside rear view mirror (OSRVM). Wind noise is the noise caused by pressure fluctuations in an unsteady flow field. Hanaoka et al. [3] found that the noise is caused by the irregular diffusion of eddy generated in the A-pillar. OSRVM is essential to secure the view of the side and rear of the car. Various studies on computational fluid dynamics (CFD) for aeroacoustics reduction around OSRVM were in progress [4-14]. In addition, there is research on vibration as well as aeroacoustics [15]. In this study, noise was predicted based on the numerical analysis results generated from OSRVM according to the change in vehicle speed. In order to predict noise through numerical analysis, it is necessary to understand the sound pressure level theory.

2. Theoretical Background

2.1. Sound Pressure Level

Sound pressure is a very small and drastic change. The magnitude of the sound pressure is defined as a sound pressure level and is calculated as a ratio to the reference sound pressure as follows.

$$SPL(f) = 10\log_{10}\left(\frac{acoustic\ pressure}{reference\ pressure}\right) = 20\log_{10}\left(\frac{p_{rms}}{p_{ref}}\right) \quad (1)$$

Here p_{ref} means a reference sound pressure. The reference sound pressure was calculated as $20\mu Pa$, which is the smallest value that humans can hear. Sound pressure waves are transmitted to the listeners at larger or offset wavelengths by mutual interface. Therefore, most of the noise can be considered as a plurality of pressure waves overlapping each wave having different frequency components and amplitudes [16]. Also, the sound pressure level has the similar meaning as the acoustic power level (APL).

2.2. Broadband Noise Source

For noise analysis, it is important to analyze the range of 20 Hz to 20,000 Hz, which is the audio frequency range. This is actually the frequency range of noise that humans can hear. Flow noise fundamentally deals with unsteady flow. The calculation of the flow field in the noise source region is completed using CFD. After that, the Ffowcs-Williams and Hawkings (FW-H) model one of the Segregated Source-Propagation Methods (SSPM) that calculates the noise propagation process is used. Noise sources should be identified more efficiently than accurate noise type and intensity analysis. However, it is important to quickly analyze the magnitude and characteristics of the approximate noise according to the shape or operating conditions too. Therefore, acoustic radiation was evaluated based on the steady Reynolds Averaged Navier Stokes (RANS) equation in this study. The APL was calculated using the Broadband Noise Source Model in ANSYS FLUENT.

3. Numerical Analysis

The model used for numerical analysis was redesigned and modelled with reference to general OSRVM. The total length of the OSRVM is 250 mm and the height is 170 mm, and the model used in this study is shown in Fig. 1 (a). For more accurate calculations around OSRVM, about 4.3×10^6 unstructured dense grids were generated based on grid dependency test. Based on the numerical analysis results of the OSRVM without groove, the part with a high APL value was modified and then modelled. The modified OSRVM has a grooved shape. The modified OSRVM is shown in Fig. 1 (b). The length between the grooves is 25mm and the number of grids is about 4.5×10^6. ANSYS FLUENT 2020 R2, which is calculated based on the finite volume method, was used For numerical analysis. The finite volume method is a method of discretizing the scalar component by convection and diffusion of each governing equation for integration using the green Gauss theorem [17].

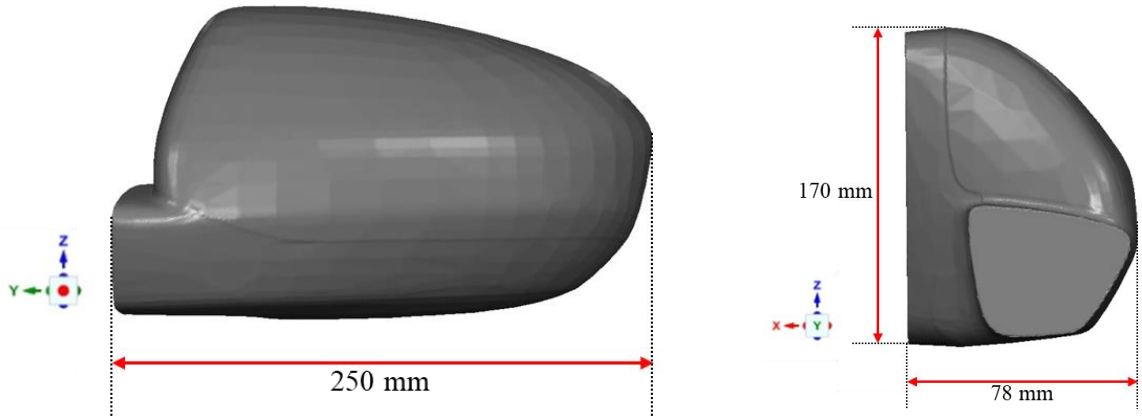

a) Geometry of the reference modelled OSRVM

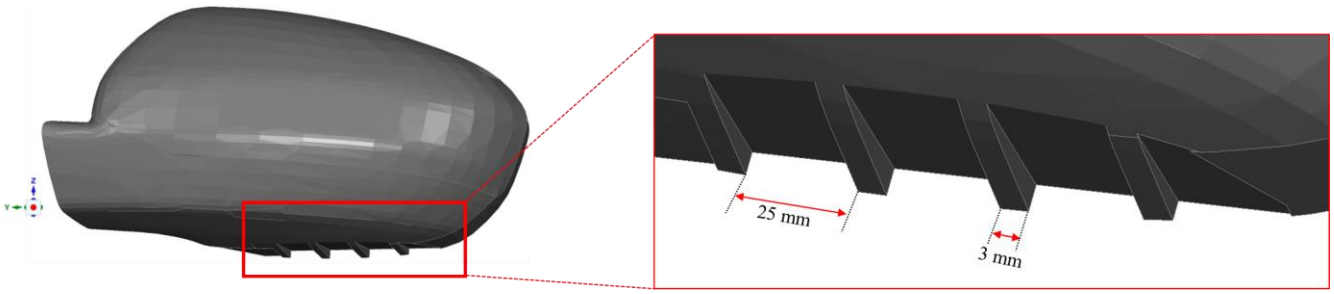

b) Geometry of the modified modelled OSRVM

Fig. 1 Geometry of the OSRVM.

3.1. Turbulence Modelling

The turbulence model applied an SST model that enables accurate calculation in complex flow phenomena and flow near the wall. The SST equation is expressed as follows.

$$\frac{D\rho k}{Dt} = \tau_{ij}\frac{\partial u_i}{\partial x_j} - \beta^*\rho\omega k + \frac{\partial}{\partial x_j}\left[(\mu + \sigma_k\mu_t)\frac{\partial k}{\partial x_j}\right] \tag{2}$$

$$\frac{D\rho\omega}{Dt} = \frac{\gamma_2}{\nu_2}\tau_{ij}\frac{\partial u_i}{\partial x_j} - \beta_2\rho\omega^2 + \frac{\partial}{\partial x_j}\left[\left(\mu + \sigma_{\omega_2}\mu_t\right)\frac{\partial \omega}{\partial x_j}\right] + 2(1-F_1)\rho\sigma_{\omega_2}\frac{1}{\omega}\frac{\partial k}{\partial x_j}\frac{\partial \omega}{\partial x_j} \tag{3}$$

$$\phi = F_1\phi_{k-\omega} + (1-F_1)\phi_{k-\varepsilon} \tag{4}$$

Here, F_1 is a blending function and has the following relationship with the model constant (ϕ).

3.2. Boundary Conditions

The fluid flowing around the OSRVM used incompressible air ($\rho = 1.225\ \mathrm{kg/m^3}$, $\mu = 1.7894 \times 10^{-5}\ \mathrm{kg/(m \cdot s)}$) and turbulence model was calculated using k-ω SST. No-slip condition was applied to the walls. The velocity inlet condition was used for the inlet of the fluid domain, and the velocity was set to a total of three different values 20, 30, and 40 $\mathrm{m/s}$. For the outlet boundary condition, 101.325 kPa was used as the atmospheric pressure condition. Detailed boundary conditions are shown in Table 1.

Table 1 Boundary conditions applied in this study

Inlet	Velocity inlet (20, 30, 40 m/s)
Outlet	Pressure outlet (101.325 kPa)
Wall	No-slip condition ($v_0 = 0\ \mathrm{m/s}$)

4. Results and Discussion

In this study, APL was calculated using the BNS Model that evaluates acoustic radiation based on steady RANS. wasting unnecessary costs in the product design phase. It is important to select an appropriate noise analysis method according to the design phase. In the final design phase, the acoustic analogy is used. Product performance verification required through acoustic experiment. Research using the BNS model is highly efficient. In this study, APL was based on the BNS model. The noise was predicted using the calculated numerical analysis results. In Fig. 2, the noise distribution for the three different driving speeds of OSRVM with and without groove was analyzed. First, it is the result of the OSRVM without groove. As the velocity increased, the APL naturally increased. On the other hand, it can be seen that the velocity increase rate and the APL increase rate are very different. When the velocity increased from 20 m/s to 30 m/s, the APL increased only by 0.01 dB. When the driving speed inlet condition changed from 30 m/s to 40 m/s, the APL increased by 24.75 dB. It is considered that this has less influence on OSRVM under conditions below a certain velocity. The highest APL in common at the bottom of the OSRVM in all velocity distributions. The highest APL is indicated by a white ball and the maximum APL results for velocity are summarized in Table 2 and 3. Second, the design of OSRVM was changed to reduce noise. The numerical analysis results of the modified modelled OSRVM with groove are as follows. When the driving speed increased by 10 m/s, the APL increased by 0.54, 0.24, and 24.93 dB. Compared to modelled OSRVM without grooves, -1.05, -0.82, and -0.64 dB decreased at driving speeds of 20, 30, and 40 m/s, respectively. The study was conducted by designing the shape of the lower part of OSRVM to reduce aerodynamic noise where high noise was predicted. The modified modelled OSRVM did not have much effect on noise reduction. In the future, research on the exact noise generation point is needed, and it is considered that there will be an optimal shape design. Additionally, we will conduct feature optimization studies for aerodynamic noise reduction.

Table 2 Comparison of APL results for OSRVM without grooves according to different driving speed condition

Driving speeds [m/s]	20	30	40
Maximum acoustic power level [dB]	76.03	76.04	100.79

Table 3 Comparison of APL results for OSRVM with grooves according to different driving speed condition

Driving speeds [m/s]	20	30	40
Maximum acoustic power level [dB]	74.98	75.22	100.15

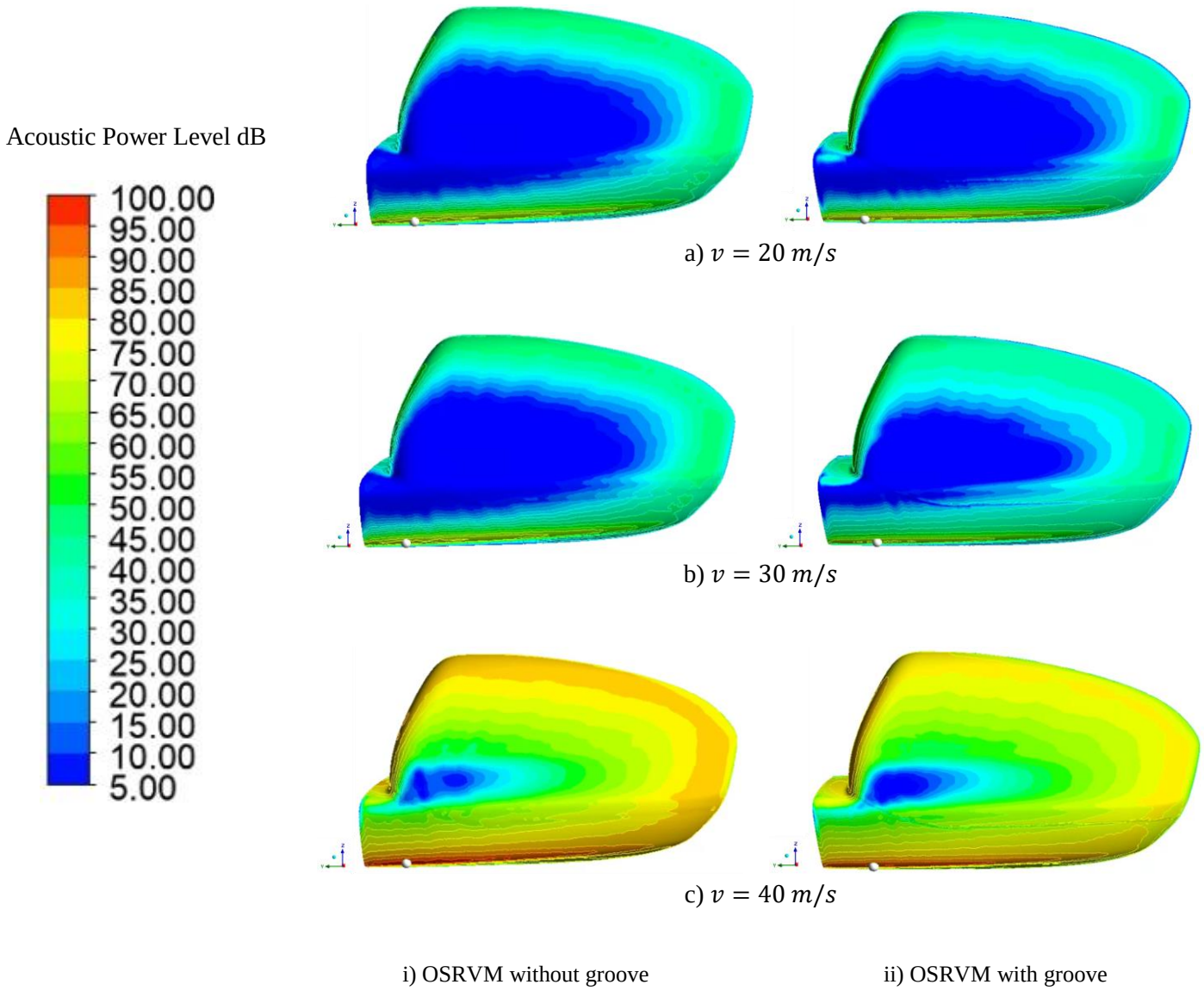

Fig. 2 APL contours for OSRVM with and without grooves according to different driving speed condition

5. Conclusion

Recently, interest in Noise, Vibration, and Harshness (NVH) for automobiles is growing. In electric vehicles without engine, customer demands for noise reduction are increasing and the importance is becoming apparent. Most of the methods to reduce the noise of products have been carried out through experiments. In this study, a noise analysis study through steady flow analysis was conducted. The noise generated from OSRVM according to the change in vehicle driving speed was predicted, and the results are summarized as follows:

1) Numerical analysis was performed on the noise predictions of the OSRVM with and without grooves. According to the driving speed conditions (20, 30, and 40 m/s), the APL difference between the two models is 1.05, 0.82, 0.64 dB.

2) The broadband noise simulation model is effective in efficiently figuring out the size and location of noise sources. We present a new method that can replace the existing research method that relied on experiments.
3) Research on aeroacoustics combining flow analysis and noise analysis has recently begun to attract attention. It is believed that it will be possible to contribute to the development of the industry by predicting noise through many studies on the visualization of aeroacoustics in the future.

References

[1] G. Keizer, *Public Affairs*. The Unwanted Sound of Everything We want: A Book about Noise, 2010.
[2] W. H. Hucho, "Aerodynamics of Road Vehicles from Fluid Mechanics to Vehicle Engineering," 4th Edn., *Society of Automotive Engineers Inc*., 1998.
[3] Y. Hanaoka, M. Zhu and H. Miyata, "Numerical Prediction of Wind Noise Around the Front Pillar of a Car-like Body," no. 931895, *SAE Technical Paper*, 1993.
[4] Y. J. Chu, Y. S. Shin and S. Y. Lee, "Aerodynamic Analysis and Noise Reducing Design of an Outside Rear View Mirror," *Applied Sciences*, 8(4), pp. 519, 2018.
[5] L. Qiliang, L. Wei, H. Xiaowei and Y. Zhigang, "Aerodynamic Noise Control of Rear View Mirror by steady and unsteady Jets," *Applied Acoustics*, vol. 192, no. 108739, 2022.
[6] M. Zaareer and A. H. Mourad, "Effect of Vehicle Side Mirror Base Position on Aerodynamic Forces and Acoustics," *Alexandria Engineering Journal*, 61(2), pp. 1437-1448, 2022.
[7] X. Chen, S. Wang, Y. Q. Wu, Y. Y. Li and H. Y. Wang, "Experimental and Numerical Investigations of the Aerodynamic Noise Reduction of Automotive Side View Mirrors," *Journal of Hydrodynamics*, 30(4), pp. 642-650, 2018.
[8] Li, Q. Yang, Z. Y. Wang and Y. He, "Experimental and Numerical Studies on Aerodynamic Noise of Automotive Rear View Mirror," *Noise Control Engineering Journal*, 59(6), pp. 613-621, 2011.
[9] J. Ye, M. Xu, P. Xing, Y. Cheng, D. Meng, Y. Tang and M. Zhu, "Investigation of Aerodynamic Noise Reduction of Exterior Side View Mirror Based on Bionic Shark Fin Structure," *Applied Acoustics*, 182, pp. 108188, 2021.
[10] M. Hartmann, J. Ocker, T. Lemke, A. Mutzke, V. Schwarz, H. Tokuno, ... and G. Wickern, "Wind Noise Caused by the Side-Mirror and A-pillar of a Generic Vehicle Model," *In 18th AIAA/CEAS Aeroacoustics Conference (33rd AIAA Aeroacoustics Conference)*, pp. 2205, 2012.
[11] C. Y. Kim, Y. W. Ban and S. H. Kim, "Shape Optimization of Side Mirror for the Reduction of Aeroacoustics," *Proceedings of the Korean Society for Noise and Vibration Engineering Conference*, pp. 117-118, 2013.
[12] C. Yu, "Automotive wind Noise Prediction Using Deterministic Aero-Vibro-Acoustics Method," *In 23rd AIAA/CEAS Aeroacoustics Conference*, pp. 3206, 2017.
[13] W. Fu and Y. Li, "Noise Control of a Rear View Mirror by Using a Slotted Base Support, *3rd International Conference on Industrial* Aerodynamics, 2021.
[14] M. Oswald and D. Caridi, "Aero-Vibro-Acoustics for Wind Noise Applications*," In 2015 Automotive Simulation World Congress*, 2015.
[15] S. Glegg and W. Devenport, "Aeroacoustics of Low Mach Number Flows: Fundamentals, Analysis, and Measurement," *Academic Press*, 2017.
[16] M. H. Zawawi, A. Saleha, A. Salwa, N. H. Hassan, N. M. Zahari, M. Z. Ramli and Z. C. Muda, "A Review: Fundamentals of Computational Fluid Dynamics (CFD)," *In AIP Conference Proceedings*, 2030(1), pp. 020252, 2018.
[17] Y. T. Kim, "Aeroacoustics Analysis by ANSYS Fluent," ANZINE, vol. 33, pp. 69-99, 2015.